Simulations of RHIC Coherent Stabilities Due to Wakefield and Electron Cooling

G.Wang, M.Blaskiewicz *BNL, Upton NY11973, USA*

Abstract

The Electron cooling beam has both coherent and incoherent effects to the circulating ion beam. The incoherent longitudinal cooling could reduce the ion beam energy spread and hence cause 'over-cooling' of the ion beam. Depending on the beam densities and cooling length, the coherent interaction between the ion and electron beam could either damp or anti-damp the ion coherent motions. Using the tracking codes, TRANFT, the threshold for 'over-cooling' has been found and compared with theoretical estimation. The transverse coherent effect of electron cooling has been implemented into the codes and its effect for the bunched ion beam is shown.

1 INTRODUCTION

Although the major task of RHIC-II electron cooling is to compensate the transverse emittance growth due to IBS, the longitudinal cooling could also happen for certain cooling schemes[1]. As a result, the energy spread of the ion beam decreases with the cooling process and may eventually destroy the Landau damping. Depending on the specific impedances of the machine, either longitudinal or transverse coherent instabilities will take place and thus cause emittance deterioration or beam loss. On the other hand, the electron beam itself can also coherently interact with the ion beam and thus affect the instability threshold and growth rate. A tracking code, TRAFT, is used to study the coherent instability of the RHIC ion beam with the coherent effects of the electron cooling being taken into account. In section 2, we describe the simulation algorithm and the impedances used for the RHIC simulation. In section 3, the simulation results are shown and the energy spread threshold for the instability is compared with analytic formula derived from the coasting beam dispersion relation. For the current 10^9 ions per bunch, when the chromaticity is set to a slightly positive value at the top energy, the longitudinal instability happens before the transverse instability as the energy spread decreasing. However this is not true for a longer bunch with the same longitudinal phase space density. For fixed bunch length and increasing particle numbers, the transverse head-tail instability happens before the longitudinal instability but its growth can be suppressed by the coherent damping effect of the electron beam, which is shown in section 4. We make conclusion in section 5.

2 TRACKING CODES DESCRIPTION

The FORTRAN program TRANFT simulates coherent instability in circular machine by using FFT logarithms. Each ion bunch is represented by $10^4 \sim 10^5$ macro particles, which are updated every turn according to the following equations[2]

$$\varepsilon_{n+1} = \varepsilon_n + \frac{q}{mc^2}\left[V_{rf}(\tau_n) - V_{s,n}(\tau_n)\right] \tag{1}$$

$$\tau_{n+1} = \tau_n + \frac{T_0 \eta}{\beta^2 \gamma_0}\varepsilon_{n+1} \tag{2}$$

$$\begin{pmatrix} x \\ p_x \end{pmatrix}_{n+1} = M_{ecool} M_{wake} M_{TWISS} \begin{pmatrix} x \\ p_x \end{pmatrix}_n \tag{3}$$

ε is the energy deviation in units of γ_0 and τ is the arrival time of the particle with respect of the synchronous particle. $V_{s,n}$ is the longitudinal voltage due to the Wakefield and is calculated by convolving the beam current with the Wakefield.

$$V_s(t) = -\int_{-\tau_b}^{\tau_b} W_s(\tau) I(t-\tau) d\tau \tag{4}$$

Equation (3) is a short hand expression for three different transverse effects. M_{TWISS} is the effect due to external focusing, which can be written as

$$M_{TWISS} \begin{pmatrix} x \\ p_x \end{pmatrix}_n = \begin{pmatrix} \cos(2\pi\nu_x) & \beta_{avg} \sin(2\pi\nu_x) \\ -\dfrac{\sin(2\pi\nu_x)}{\beta_{avg}} & \cos(2\pi\nu_x) \end{pmatrix} \begin{pmatrix} x - \delta_n D_x \\ p_x \end{pmatrix}_n + \delta_{n+1} \begin{pmatrix} D_x \\ 0 \end{pmatrix} \tag{5}$$

, where $\delta_n = \dfrac{\varepsilon_n}{\gamma_0 - \gamma_0^{-1}}$ and $\nu_x = \nu_{x,0} + \xi_x \delta_n$. M_{wake} is the transverse kick due to Wakefield and can be calculated by convolving the dipole momentum of the beam with the transverse Wakefield.

$$M_{wake} \begin{pmatrix} x \\ p_x \end{pmatrix} = \begin{pmatrix} x \\ p_x + \Delta p_x \end{pmatrix} \tag{6}$$

$$\Delta p_x = -\int_{-\tau_b}^{\tau_b} W_x(\tau) D(t-\tau) d\tau \tag{7}$$

The dipole momentum is defined as $D(t) \equiv I(t)\langle x(t) \rangle$. In principal, one can directly apply equation (4) and (7) to sum up the contribution from each macro-particle. However the amount of calculations can be greatly reduced by placing the macro-particles in an evenly distributed grids and use FFT technique to calculate the longitudinal and transverse voltages. Since the convolution in time domain is equivalent to multiply in the frequency domain, the Wakefield is transformed into Impedance, multiplied by the Fourier component of the current and then transformed back to the time domain to get the voltages for each grid point. In order to obtain the kicks for each macro-particle, linear interpolation is applied between the grids. The resistive wall impedance was estimated by the low frequency formula

$$Z_\perp(\omega) = [1 - i\,\mathrm{sgn}(\omega)] \frac{Z_0 R \delta_{skin}}{b^3} \tag{8}$$

$$Z_{//}(\omega) = [1 - i\,\mathrm{sgn}(\omega)] \frac{Z_0 \delta_{skin}}{2b} \frac{\omega}{\omega_0} \tag{9}$$

, where $\delta_{skin} \equiv \sqrt{\dfrac{c}{Z_0 \sigma \omega}}$, $b \approx 3cm$ and $\sigma \approx 1.39 \times 10^6 \Omega^{-1} m^{-1}$ are the skin depth, radius and conductivity of the wall respectively. $Z_0 \equiv 377\Omega$ is the impedance of the free space, $R \approx 610m$ is the average radius of RHIC. The transverse space charge impedance was calculated by the following formula

$$Z_{\perp sc} = \frac{Z_0 R}{\beta^2 \gamma^2 a^2} \tag{10}$$

, where $a = 2\sigma_b$ is the radius of equivalent uniform beam. The impedance due to bellows and abort kicker are approximated by RLC resonant circuits model[3].

$$Z_{\perp BB} = \frac{R_{sh}}{1 + iQ\left(\frac{\omega_r}{\omega} - \frac{\omega}{\omega_r}\right)} \frac{\tilde{\omega}}{\omega} \tag{11}$$

, where $\tilde{\omega} = \omega_r \sqrt{1 - \frac{1}{4Q^2}}$ is the oscillation frequency of the wake field. The parameters of the considered broad band impedances are listed in Table 1. The inductive longitudinal impedance of

	Q	$R_{sh}(M\Omega \cdot m^{-1})$	f_r (MHz)
Bellows	1.74	1.00	5.2×10^3
Abort Kicker	0.66	1.05	46.3

Table 1. Parameters for Transverse Broad Band Impedance

RHIC was measured to be $\frac{Z_{//}}{n} = 3j\Omega$[4]. In order to implement it into the simulation, longitudinal resonant model was assumed with test parameters $Q = 2$ and $f_r = 2GHz$.

$$Z_{// BB} = \frac{R_{sh}}{1 + iQ\left(\frac{\omega_r}{\omega} - \frac{\omega}{\omega_r}\right)} \tag{12}$$

The shunt impedance is determined by requiring equation (12) giving the measured $3j\Omega$ at the low frequency limit.

$$R_{sh} = iQ \frac{Z_{//}}{n} \frac{\omega_r}{\omega_{rev}} \approx 1.53\times10^5 \Omega \tag{13}$$

Since the beam distribution in the frequency domain is below $0.5GHz$, the simulation was not sensitive to the test parameters. The impedance from the BPMs are approximated by the following form

$$Z_{\perp bpm}(\omega) = \frac{R_{sh}}{i\frac{\omega}{\alpha_r} - 1} \tag{14}$$

, where $R_{sh} = 9.17\times10^5 \Omega \cdot m^{-1}$ and $\alpha_r = 6.54\times10^8 s^{-1}$. It corresponds to an exponentially decay wake in the time domain and gives a smoother impedance in the frequency domain as shown in Figure 1a. The longitudinal and transverse impedance are plotted in Figure 1. M_{ecool} in equation (3) is due to the long range interaction with the electron cooling beam. For non-magnetized electron cooling[5],

$$\begin{aligned} M_{ecool}\begin{pmatrix} x \\ p_x \end{pmatrix} = & \begin{pmatrix} \xi_{ie}(\cos\psi_{coh} - 1) + 1 & \frac{1}{k_{coh}}\left[\xi_{ie}\sin\psi_{coh} + (1-\xi_{ie})\psi_{coh}\right] \\ -\xi_{ie}k_{coh}\sin\psi_{coh} & \xi_{ie}(\cos\psi_{coh} - 1) + 1 \end{pmatrix} \begin{pmatrix} \langle x \rangle \\ \langle p_x \rangle \end{pmatrix} \\ & + \begin{pmatrix} \cos\psi_{inc} & \frac{1}{k_{inc}}\sin\psi_{inc} \\ -k_{inc}\sin\psi_{inc} & \cos\psi_{inc} \end{pmatrix} \begin{pmatrix} x - \langle x \rangle \\ p_x - \langle p_x \rangle \end{pmatrix} \end{aligned} \tag{15}$$

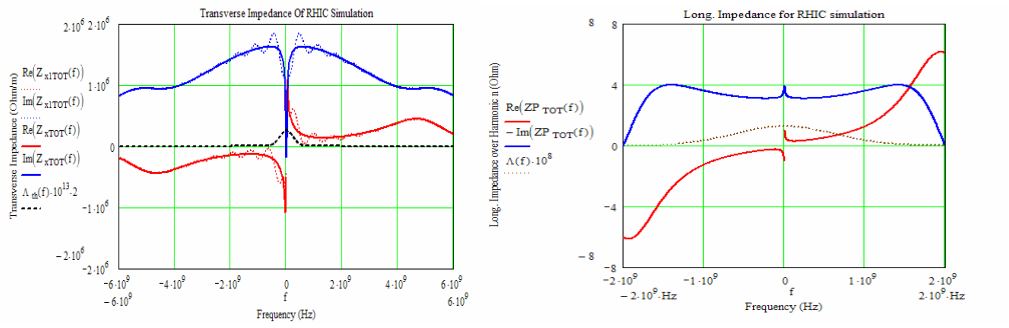

a b

Figure 1 (a) Transverse Impedance used for RHIC simulation. The red solid curve is the real part of the transverse impedance and the solid blue curve is the imaginary part of the transverse impedance. The dot blue and dot red shows the impedance when step form for BPMs wake being applied. The black dash curve shows the beam distribution. (b) Longitudinal Impedance used in RHIC simulation. The red solid curve and the blue solid curve are the real and imaginary parts of the longitudinal impedance over n respectively. The brown dot curve shows the equivalent Gaussian beam distribution in the frequency domain.

, where $\xi_{ie} \equiv \left(\frac{k_{inc}}{k_{coh}}\right)^2$. The coherent and incoherent wave number of the interaction are defined as

$$k_{inc} = \frac{1}{\beta c}\sqrt{\frac{Z_i e^2}{2\varepsilon_0 \gamma^3}\frac{n_e}{M_i}} \tag{16}$$

$$k_{coh} = \frac{1}{\beta c}\sqrt{\frac{Z_i e^2}{2\varepsilon_0 \gamma^3}\left(\frac{n_e}{M_i}+\frac{n_i}{m_e}\right)} \tag{17}$$

Accordingly, the coherent and incoherent phases advance over the cooling section are given by $\psi_{coh} \equiv k_{coh} l_{cool}$ and $\psi_{inc} \equiv k_{inc} l_{cool}$.

3. SIMULATION RESULTS

Since the rf voltage and harmonic number were kept the same for all simulations, the momentum spread was always proportional to the bunch length. In order to investigate the momentum spread threshold of overcooling, the initial bunch length was gradually reduced from its current operational value $\sigma_s \approx 20cm$ until either longitudinal or transverse instability was observed. Table 2 shows the beam parameters we used for the simulation. About 10^5 macro-particles were tracked during the simulation. The initial longitudinal distribution was parabolic and the initial rf voltage was linear. The beam was

Beam Energy γ	100
Beam Particle	Au^{79+}
Transverse rms Emittance ε_x ($\pi \cdot mm \cdot mrad$)	4.2
Bunch Population	10^9
RF Voltage (MV)	3
RF Harmonic number	2520
Chromaticity ξ_x	2

Table 2 Parameters for RHIC coherent instability simulation

adiabatically matched to a sinusoidal rf voltage within 1000 turns. As shown in Figure 3a, for initial $\delta p / p \le 1.4\times10^{-4}$ the longitudinal emittance started to grow rapidly. After a few hundreds turns, the momentum spread increased well above the stability threshold and the growth was suppressed as the beam reached to its new equilibrium. Figure 2b shows the longitudinal beam profile after 5000 turns. As one can see the coherent oscillation

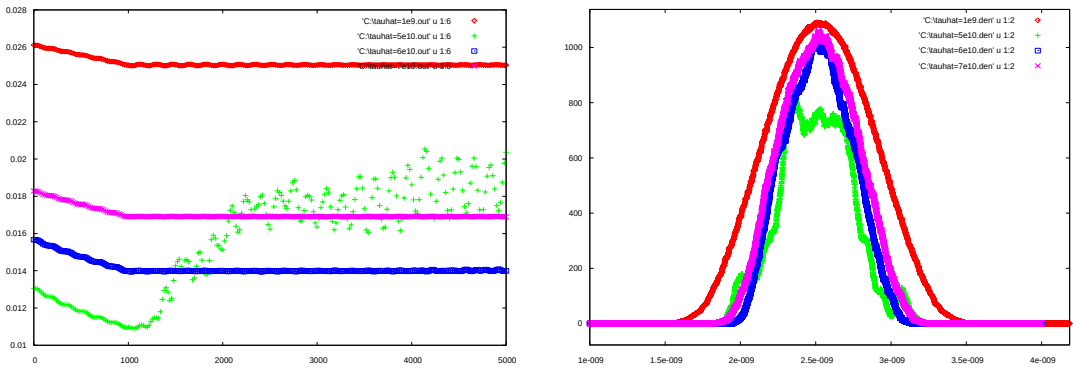

(a) (b)

Figure 2 (a) Momentum spread evolution for chromaticity $\xi_x = 2$. The horizontal axis is the number of turns being simulated and the vertical axis is the momentum spread $\delta p / p$ in unit of γ. The decreasing before 1000 turn is due to the mismatch of the longitudinal phase space. Each curve has different initial bunch length and momentum spread as shown; (b) Longitudinal beam profiles after 5000 turns. Each curve shows the longitudinal beam profile for corresponding curve in Figure 3. The horizontal axis is longitudinal position along the bunch and the vertical axis is the macro-particle density.

was still pretty strong although it was not growing anymore. There were no transverse coherent oscillation growths observed for 10^9 ions per bunch and $\xi_x = 2$ as shown in Figure 5. The coherence of a bunch is defined as the following

$$coherence = \frac{\int I(t)\left(\langle x\rangle^2 + \langle p_x\rangle^2\right)dt}{\int I(t)dt} \tag{18}$$

, where $\langle x\rangle$ and $\langle p_x\rangle$ are the average position and transverse angle for the slice $[t, t+dt]$ and the integration is over the whole bunch. From Figure 3 and Figure 5, we see that the longitudinal microwave instability happens before the transverse instability for the current operational parameters. The instability threshold was found to be $\sigma_{p,sim} \approx 1.4\times10^{-4}$, which is a factor of 3 smaller than the current momentum spread. During the simulation, the longitudinal oscillation built up very fast (less than 100 turns) and the wavelengths of the perturbation were usually smaller than the bunch length. Since the synchrotron oscillation was slower than the coherent oscillation growth rate, the dispersion relation for a coasting beam should be able to estimate the instability threshold. For the parabolic distributed beam, the dispersion relation is[6]

$$\frac{Z_{//}(\omega)}{n} = \left[i\Lambda_{//} \int_{-1}^{1} \frac{x}{x + x_1} dx \right]^{-1} \tag{19}$$

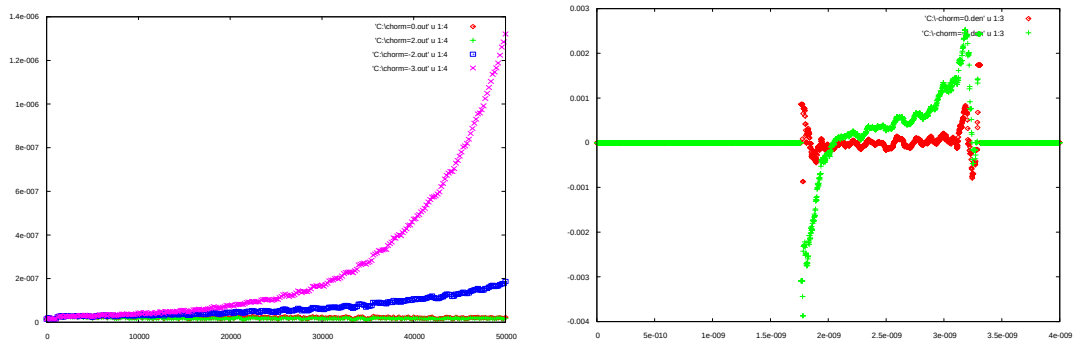

(a) (b)

Figure 3 (a) The transverse coherence evolution for varies chromaticity. The red and green curves are for $\xi_x = 0,2$ respectively. The blue and purple curves are for $\xi_x = -2$ and $\xi_x = -3$. The horizontal axis is the simulation time in units of turns and the vertical axis is the coherence as defined in equation (18); (b) The side view of the beam after 5000 turns. The horizontal axis is the longitudinal position along the beam in unit of seconds and the vertical axis is the transverse displacement in units of meter. The red curve is for $\xi_x = 0$ and the green curve is for $\xi_x = -3$

, where $\Lambda_{//} = \frac{3Z_i e I_{peak}}{2\pi\eta m_i c^2 \gamma_0 \beta_0^2 (\delta p/p)^2_{FWHH}}$ and $x_1 = \frac{\sqrt{2}\Delta\omega_{//}}{n\omega_0|\eta|(\delta p/p)_{FWHH}}$. $(\delta p/p)_{FWHH}$ is the full width half height of the momentum spread which is related to the rms momentum spread by $\sigma_p = \frac{(\delta p/p)_{FWHH}}{2\sqrt{2\ln 2}}$ and $\Delta\omega_{//}$ is the complex coherent tune shift. The solution of Equation 18 is plotted into the impedance plane as shown in Figure 6. The instability threshold can be determined by the Keil-Schnell criteria.

$$\sigma_{p,th} = \sqrt{\frac{(Z_{//}/n) I_{peak} Z_i e}{(2\ln 2) m_i c^2 \gamma_0 \beta_0^2 |\eta|}} = 1.5\times 10^{-4} \tag{20}$$

In the calculation of Equation 20, we used the peak current directly obtained from the simulation, $I_{peak} \approx 18A$. Comparing Equation 20 with the simulation results, we see that the agreement is within 10%. Since the chromaticity was set to 2, the rigid head-tail mode ($\mu = 0$) was damped. As we can see from Figure 5a, when the chromaticity was set to negative, the head-tail instability took place and the growth rate was proportional to the absolute value of the chromaticity as expected from theory. Because of the non-linear component of the rf voltage and the wake field, the higher order head-tail modes were actually landau damped by the synchrotron tune spread. As the number of particle inside the bunch increasing, the landau damping would eventually cease and for weak coupling and short bunch, the threshold can be estimated by the following dispersion relation[7]

$$Z_{eff} = \left[i \frac{ecI_{av}}{2E\omega_y} \left(\frac{1}{2^{|\mu|}|\mu|!} \right)^{2|\mu|} \left(\frac{2\eta}{\beta_0^2 E_0} \right)^{|\mu|} \int_0^\infty dH_s \left(\frac{H_s}{\nu_s(H_s)^2} \right)^{|\mu|} \frac{\psi_0(H_s)}{(Q_R - \mu\nu_s(H_s) + iQ_I)} \right]^{-1} \tag{21}$$

, where $Q \equiv Q_R + iQ_I = \frac{\Omega + \omega_y}{\omega_0}$ is the coherent tune shift and the longitudinal synchrotron oscillation Hamiltonian is defined as

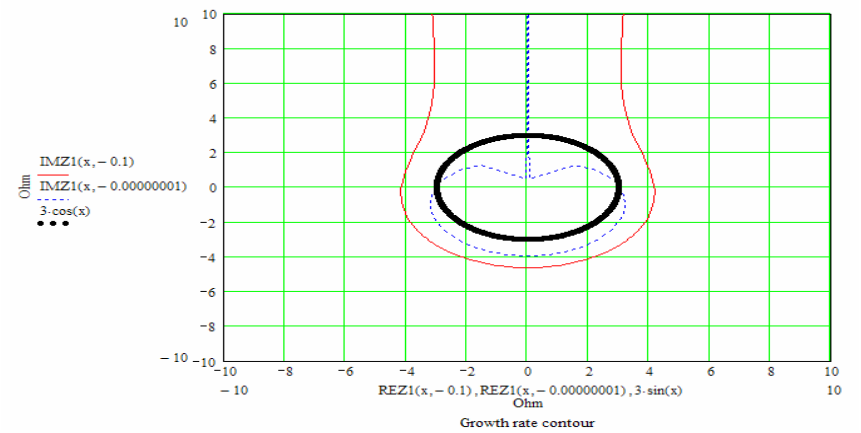

Figure 4 The growth rate contour in the normalized impedance plane for $\sigma_p = 1.7\times10^{-4}$. The horizontal and vertical axes are $\mathrm{Re}(Z_{//}/n)$ and $\mathrm{Im}(Z_{//}/n)$ respectively. The red solid curve is the contour for $\mathrm{Im}(x_1) = -0.1$ and the blue dot line is the instability threshold contour. The black solid circle is for $|Z_{//}/n| = 3ohm$.

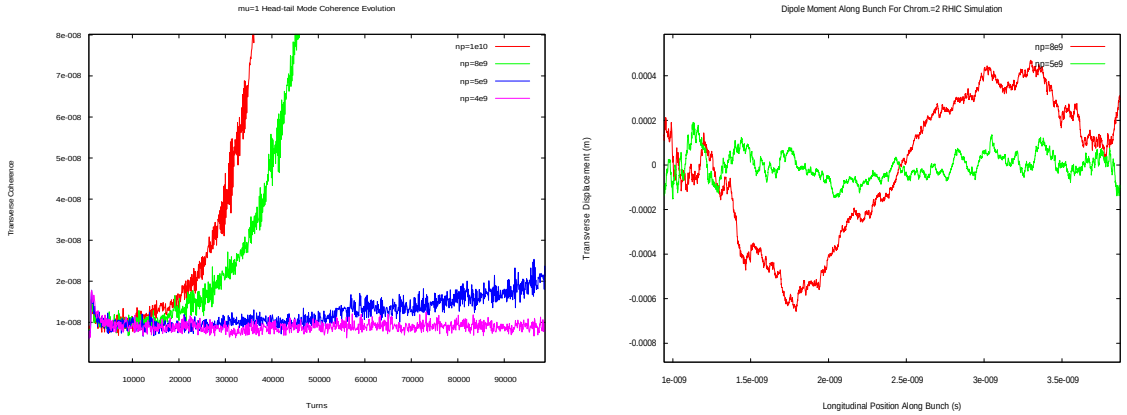

Figure 5 (a) The transverse coherence evolution for $\mu = 1$ Head-tail mode. The horizontal axis is simulation time in unit of turns and the vertical axis is the coherence as defined in Equation (18). The red green blue and purple curve are for bunch population of $10^{10}, 8\times10^9, 5\times10^9$ and 4×10^9 respectively. (b) A snapshot of the transverse displacement along the bunch. The red and green curves are for 8×10^9 and 5×10^9 ions per bunch. The green curve is taken after 10^5 turns and red is taken after 5×10^4 turns.

$$H_s \equiv \frac{1}{2}\left(\frac{e\omega_0\left|V_{rf}\cos(\varphi_s)\right|}{2\pi E_0\beta_0^2}(\varphi-\varphi_s)^2 + h\omega_0\eta\delta^2\right)\cdot\frac{E_0\beta_0^2}{h\omega_0} \tag{22}$$

The effective impedance Z_{eff} is defined as

$$Z_{eff} \equiv \sum_{n=-\infty}^{\infty}\left(n - Q_y + \frac{\xi_x}{\eta}Q_y\right)^{2|\mu|} Z\left(n\omega_0 - \omega_y + \mu\omega_{s0}\right) \tag{23}$$

The simulation result for $\xi_x = 2$ is shown in Figure 5. As the bunch population going beyond 5×10^9, the transverse motion became unstable and the growth rates were in order

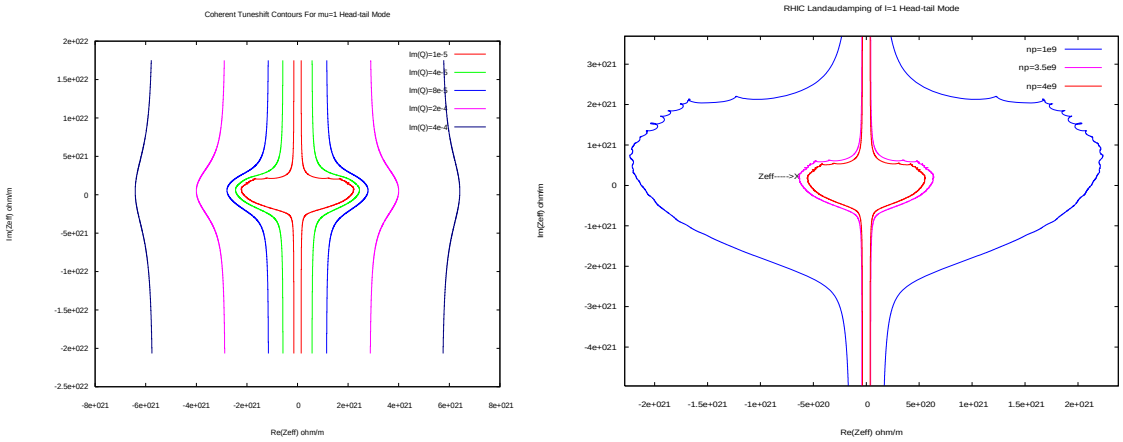

a b

Figure 6 (a) Coherent tune shift contours for $\mu = 1$ Head-tail mode. The horizontal and vertical axes are the real and imaginary part of the effective impedance in Equation (22). The bunch population is 5×10^9 and each curve corresponds to a specific growth rate; (b) Stability threshold contours for $\mu = 1$ Head-tail mode. The blue, purple and red curve are the stability threshold contours for bunch population of, 10^9, 3.5×10^9 and 4×10^9 respectively. The 'X' marks the value calculated directly from the definition, Equation (23), using the impedance shown in Figure 1.

of 10^{-5} per turn, which is consistent with the solution of dispersion relation as shown in Figure 6a. Figure 5 indicates that the unstable mode is for $m = 1, \mu = 1$ head-tail mode and the threshold for the instability should be between $n_p = 4\times10^9$ and $n_p = 5\times10^9$. Numerical solutions of the dispersion relation, i.e., equation (21), are shown in Figure 6a. As shown in Figure 6b, the instability threshold prediction from the dispersion relation is $n_p \approx 3.5\times10^9$, which agrees with the simulation result within 30%. When the beam is stable, the usually weak coherent interaction between electron cooling beam and ion beam does not play any role except for a tiny coherent tune shift. However, the slow higher order head-tail instability growth could be suppressed by the coherent force exerted by the electron beam. As shown in Figure 7, the coherent damping effect of the electron beam is small for the current electron cooler design but can be increased dramatically by increase the cooling section length since the damping rate is proportional to $l_{ecool}{}^4$. In addition to the stability problems, having more particles within the bunch

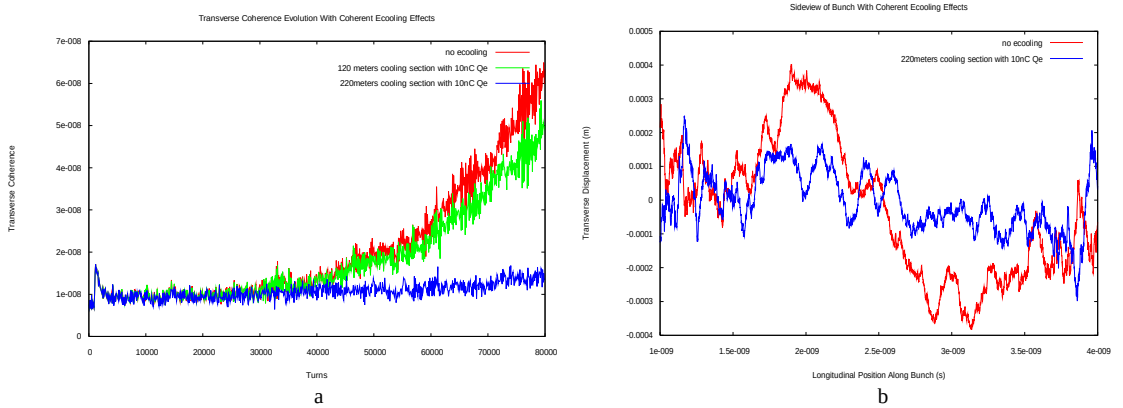

a b

Figure 7 (a) The Transverse Coherence Evolution With Varies E-cooling Parameters. The bunch population is 6×10^9 and the chromaticity is 2. (b) The Side View of The Bunch After 8×10^4 turns. The vertical axis is the coherent transverse angle multiplied by the average Beta function and the horizontal axis is the longitudinal position along the bunch.

would increase the IBS rate and thus cause the emittance deterioration, which also require higher electron charge and longer cooling section.

4. CONCLUSION

The single bunch simulation shows that the longitudinal microwave instability threshold can be accurately estimated by the coasting beam formula and for the current operational beam parameters, the threshold was found to be $\delta p / p \approx 1.5 \times 10^{-4}$. The transverse motion is stable for $\xi_x = 2$ and $n_p \le 4 \times 10^9$. High order head tail instability will occur if the bunch population is beyond the Landau damping threshold determined by the synchrotron frequency spread. The growth rate of $\mu = 1$ head tail mode is in the order of $10^{-5} \sim 10^{-4}$. This slow growth can be suppressed by the coherent force exerted by the cooling electron beam and in order to increase the head-tail threshold substantially, the length of the cooling section has to be at least 200 meters.

ACKNOWLEDGEMENTS

Thanks to Ilan Ben-zvi for suggesting this subject and to Alexei Fedotov for very useful discussions.

REFERENCES

[1] Alexei Fedotov, (2007). http://www.bnl.gov/cad/ecooling/docs/PDF/Electron_Cooling.pdf
[2] M.Blaskiewicz, The Tranft User's Manual (2006).
[3] W.MacKay eds. S.Peggs, in *RHIC/AP/36*, edited by S.Peggs (1994).
[4] J.M.Brennan M.Blaskiewicz, P.Cameron,W.Fischer, in *EPAC 2002* (Paris,France, 2002), pp. 1488.
[5] G.Wang, in *COOL05 Workshop* (AIP, Galena,Illinois, USA, 2005), Vol. 821, pp. 164.
[6] J.L.Laclare, in *CERN Accelerator School:5th General Accelerator Physics Course* (Jyvaskyla, Finland, 1992), pp. 349.
[7] Jiunn-Ming Wang, in *AIP Conference Proceedings* (1987), Vol. 153, pp. 697.